

Dynamical Stability of Cantilevered Pipe Conveying Fluid with Inerter-Based Dynamic Vibration Absorber

Zhiyuan Liu^{1,2}, Xin Tan², Xiaobo Liu^{1,2}, Pingan Chen^{1,2}, Ke Yi^{1,2}, Tianzhi Yang^{1,2}, Qiao Ni^{3,4} and Lin Wang^{3,4,*}

¹The State Key Laboratory of Heavy Duty AC Drive Electric Locomotive Systems Integration, Zhuzhou, 412001, China

²CRRC Zhuzhou Locomotive Co., Ltd., Zhuzhou, 412001, China

³Department of Mechanics, Huazhong University of Science and Technology, Wuhan, 430074, China

⁴Hubei Key Laboratory for Engineering Structural Analysis and Safety Assessment, Wuhan, 430074, China

*Corresponding Author: Lin Wang. Email: wanglinds@mail.hust.edu.cn

Received: 11 June 2020; Accepted: 07 August 2020

Abstract: Cantilevered pipe conveying fluid may become unstable and flutter instability would occur when the velocity of the fluid flow in the pipe exceeds a critical value. In the present study, the theoretical model of a cantilevered fluid-conveying pipe attached by an inerter-based dynamic vibration absorber (IDVA) is proposed and the stability of this dynamical system is explored. Based on linear governing equations of the pipe and the IDVA, the effects of damping coefficient, weight, inerter, location and spring stiffness of the IDVA on the critical flow velocities of the pipe system is examined. It is shown that the stability of the pipe may be significantly affected by the IDVA. In many cases, the stability of the cantilevered pipe can be enhanced by designing the parameter values of the IDVA. By solving nonlinear governing equations of the dynamical system, the nonlinear oscillations of the pipe with IDVA for sufficiently high flow velocity beyond the critical value are determined, showing that the oscillation amplitudes of the pipe can also be suppressed to some extent with a suitable design of the IDVA.

Keywords: Cantilevered pipe conveying fluid; inerter-based dynamic vibration absorber; dynamic vibration absorber; critical flow velocity; nonlinear oscillation

1 Introduction

The dynamical stability of cantilevered pipes conveying fluid has been widely studied by many researchers [1–6] in the past decades. The main reason why so many people are devoting on this problem is because the dynamical system of pipes conveying fluid can be found in many engineering fields, such as, heat exchanger tubes, concrete pump truck, locomotive braking system, oil pipeline, aerial refueling, ocean risers, and etc.

It is generally known that a cantilevered pipe may become unstable and flutter instability would occur when the velocity of the fluid flow in the pipe exceeds a critical value. Indeed, a lot of researchers have endeavored to enhance the stability of cantilevered pipes conveying



This work is licensed under a Creative Commons Attribution 4.0 International License, which permits unrestricted use, distribution, and reproduction in any medium, provided the original work is properly cited.

fluid [7–17], by using either passive or active methods. For instance, Tani et al. [12,13] applied a torsional moment to a certain position of the cantilevered fluid-conveying pipe, and then experimentally and numerically studied the suppression effect of the torque on the oscillation responses of the pipe. Yau et al. [2] added a piezoelectric layer to a certain position of the cantilevered pipe, and explored the effect of the mounting position and the length of the piezoelectric layer on the vibration responses of the pipe. Lin et al. [9,14,15] further demonstrated that the cantilevered pipe could obtain remarkable suppression effect when the voltage imposed on the piezoelectric layer was within a suitable range. Khajepour et al. [16] utilized piezoelectric layers to control the vibrations of a rotating cantilever conveying fluid. Hussein et al. [17] analyzed the effect of hydraulic damper position, base width of hydraulic damper, damping and flow pressure on the dynamic responses of slender pipes by using state space technique.

Since active control methods for cantilevered pipes conveying fluid are always restricted by the reliability and service life of the controller, passive control methods [18–22] have attracted more attentions. For instance, Wang et al. [23] derived the governing equations of a pipe conveying fluid on elastic foundation and showed that an elastic foundation can increase the critical flow velocity for static and dynamical instabilities of the pipe. Doaré et al. [24] compared the stability characteristics of finite- and infinite-length pipes conveying fluid on elastic foundations. Hiramoto et al. [20] improved the stability of cantilevered pipes conveying fluid by optimizing the outer diameter distribution of the pipe with a closed-loop device. Pisarski et al. [25] applied electromagnetic devices of a motional type to cantilevered pipes conveying fluid to improve the dynamical stability of the pipe system. It was demonstrated that the electromagnetic devices of the motional type can remarkably increase the critical flow velocity by fifty percent comparing to the same pipe but without the electromagnetic actuator.

At the year of 2013, Yang et al. [26] initiated to numerically investigate the nonlinear responses of simply supported pipes conveying fluid with an attached nonlinear energy sink (NES). A cubic spring linked with a mass was used to model the effect of NES on the pipe system. It was indicated that the vibrational energy of the simply supported pipe conveying fluid could be robustly absorbed by the NES. Based on the work of Yang et al. [26], Mamaghani et al. [27] used an attached NES to suppress the oscillation responses of clamped–clamped pipe conveying fluid subjected to an external harmonic force. It was demonstrated that the pipe could achieve excellent suppression effect by attaching the NES at the middle point of the pipe. Song et al. [28] explored the vibration control performance of a Pounding Tuned Mass Damper (PTMD) for pipe structures by installing a PTMD on an M-shaped pipeline, using both experimental and numerical methods. Rechenberger et al. [29] used Microsoft Excel spreadsheet calculations to establish a mathematical model of Tuned Mass Damper (TMD). Their studies were of a practical guidance on the design of TMD for suppressing the oscillations of pipeline structures. Zhou et al. [30] installed an NES attachment somewhere along the length of a cantilevered pipe conveying fluid to enhance the stability of the pipe. The effects of mass ratio, spring stiffness, damping and location of the NES on the stability and nonlinear responses of the pipe were explored. Very recently, Liu et al. [31] analyzed the dynamical stability of a cantilevered pipe with an additional linear dynamic vibration absorber (DVA) attachment. It was shown that the damping coefficient, spring stiffness, location and weight of the DVA can remarkably affect the dynamical behaviors of the pipe.

In the current work, we introduce an inerter-based dynamic vibration absorber (IDVA) [32–35] to adjust the dynamical stability of cantilevered pipes conveying fluid. Based on the proposed governing equations, the effect of several key parameters of the additional IDVA

on the dynamics of the pipe are investigated. It will be shown that the IDVA can enhance the stability and suppress the oscillations of the pipe in many cases.

2 Governing Equations

Fig. 1 shows the schematic diagram of a cantilevered pipe conveying fluid with an additional IDVA. The spring-mass attachment is attached at $x = x_b \leq L$, where L is the pipe length. The pipe is horizontal and its motion is limited in a horizontal plane by embedded a steel strip in the pipe.

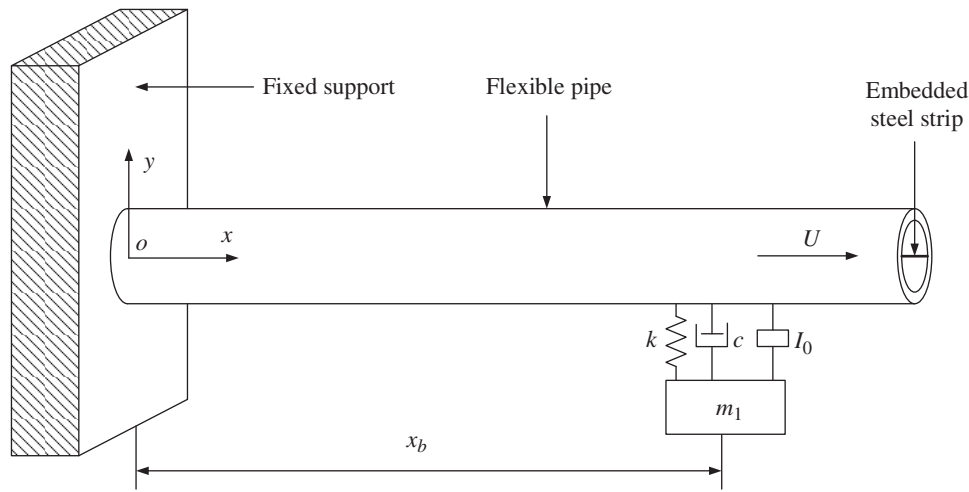


Figure 1: Schematic of a cantilevered pipe subjected to an inerter-based dynamic vibration absorber

In Fig. 1, the lateral displacement of the pipe along the y axis is denoted by $W(s, t)$, with s being the curvilinear coordinate along the pipe length and t being the time. Before giving the nonlinear governing equations of the pipe system, several basic assumptions were made [36,37]: (1) The internal axial fluid is incompressible; (2) The centreline of the pipe is inextensible; (3) The Euler–Bernoulli beam theory is acceptable for the pipe; (4) The pipe’s axial strain is sufficiently small, although its lateral deflection may be relatively large. Following the derivation of Semler [38] and Liu et al. [31] and considering the effect of IDVA, the equation of motion of the pipe may be written as

$$\begin{aligned}
 & (m + M) \ddot{W} + 2MU\dot{W}'(1 + W'^2) + MU^2(1 + W'^2)W'' + \psi IW'''' \\
 & + EI \left[W''''(1 + W'^2) + 4W'W''W'''' + W''^3 \right] + W' \int_0^s (m + M) (\dot{W}'^2 + W'\ddot{W}'') ds \\
 & - W'' \left[\int_s^L \int_0^s (m + M) (\dot{W}' + W'\ddot{W}'') ds ds + \int_s^L (2MUW'\dot{W}' + MU^2W'W'') ds \right] \\
 & - [K(V - W_b) + C(\dot{V} - \dot{W}_b) + I_0(\ddot{V} - \ddot{W}_b)] \delta(s - s_b) = 0
 \end{aligned} \tag{1}$$

in which the overdots and primes denote the derivative with respect to t and s , respectively; ψ is the Kelvin–Voigt damping coefficient of the pipe, EI is the flexural rigidity of the pipe; m is

the mass of the empty pipe per unit length, U is the steady flow velocity, M is the mass of the internal fluid per unit length; W_b is the lateral deflection of the pipe at the location of the IDVA attachment; C is the damping coefficient of the damper, K is the stiffness of the spring, I_0 denotes the inerter of the IDVA, V is the displacement of the additional mass; $\delta(s - s_b)$ is the Dirac delta function with s_b being the location of the IDVA.

The governing equation of the IDVA takes the form

$$m_1 \ddot{V} + K(V - W_b) + C(\dot{V} - \dot{W}_b) + I_0(\ddot{V} - \ddot{W}_b) = 0 \quad (2)$$

where m_1 is the mass of the attached rigid body.

Introducing the following dimensionless quantities

$$\begin{aligned} \xi = \frac{s}{L}, \quad w = \frac{W}{L}, \quad v = \frac{V}{L}, \quad \tau = \left(\frac{EI}{m+M} \right)^{1/2} \frac{t}{L^2}, \quad u = \left(\frac{M}{EI} \right)^{1/2} UL, \quad \beta = \frac{M}{M+m}, \\ \phi = \left(\frac{EI}{m+M} \right)^{1/2} \frac{\psi}{L^2}, \quad \alpha = \frac{m_1}{(M+m)L}, \quad k = \frac{KL^3}{EI}, \quad \gamma = \frac{m+M}{EI} L^3 g, \quad c = \frac{CL}{[(m+M)EI]^{1/2}}, \\ \theta = \frac{I_0}{(M+m)L} \end{aligned}$$

Eqs. (1) and (2) may be written in dimensionless forms as

$$w'''' + \phi \dot{w}'''' + \ddot{w} + 2u\sqrt{\beta} \dot{w}' + u^2 w'' + N(w) - [k(v - w_b) + c(\dot{v} - \dot{w}_b) + \theta(\ddot{v} - \ddot{w}_b)] \delta(\xi - \xi_b) = 0 \quad (3)$$

and

$$\alpha \ddot{v} + k(v - w_b) + c(\dot{v} - \dot{w}_b) + \theta(\ddot{v} - \ddot{w}_b) = 0 \quad (4)$$

where the prime and overdot on each variable now denote the derivative with respect to ξ and τ , respectively. The nonlinear term $N(w)$ in Eq. (3) is given by

$$\begin{aligned} N(w) = 2u\sqrt{\beta} \dot{w}' w'^2 + w'' u^2 w'^2 + 3w' w'' w''' + w''^3 + w' \int_0^\xi \left\{ \dot{w}'^2 - 2u\sqrt{\beta} w' \dot{w}'' - u^2 w' w'''' + w'' w'''' \right\} d\xi \\ - w'' \int_\xi^1 \int_0^\xi \left[\dot{w}'^2 - 2u\sqrt{\beta} w' \dot{w}'' - u^2 w' w'''' + w'' w'''' \right] d\xi d\xi \\ - w'' \int_\xi^1 \left(2u\sqrt{\beta} w' \dot{w}' + u^2 w' w'' + w'' w'''' \right) d\xi \end{aligned} \quad (5)$$

3 Galerkin Discretization

The governing equations for the pipe and IDVA are in partial differential forms, which can be discretized by using several effective methods including Galerkin approach [39–41] and differential quadrature method [42–44]. In the following calculations, the Galerkin approach is used to discretize the partial differential equations. Based on this method, the displacements of the pipe can be given by

$$w(\xi, \tau) = \sum_{r=1}^N \varphi_r(\xi) q_r(\tau) \quad (6)$$

where $\varphi_r(\xi)$ is the base eigenfunctions of a plain cantilevered beam, and $q_r(\tau)$ is the corresponding generalized coordinates; N is the number of base functions used in the discretization. Substituting expression (6) into Eqs. (3) and (4), multiplying by $\varphi_i(\xi)$ and integrating from 0 to 1, the following ordinary differential equations can be obtained

$$[\mathbf{M}] \begin{Bmatrix} \ddot{\mathbf{q}} \\ \ddot{\mathbf{v}} \end{Bmatrix} + [\mathbf{C}] \begin{Bmatrix} \dot{\mathbf{q}} \\ \dot{\mathbf{v}} \end{Bmatrix} + [\mathbf{K}] \begin{Bmatrix} \mathbf{q} \\ \mathbf{v} \end{Bmatrix} + \{\mathbf{f}_{nonl}\} = \{\mathbf{0}\} \quad (7)$$

where the overdots now denote the total derivative with respect to dimensionless time τ . In Eq. (7), $[\mathbf{M}]$, $[\mathbf{C}]$ and $[\mathbf{K}]$ represent the mass, damping and stiffness matrices for the linear parts and \mathbf{f}_{nonl} denotes the nonlinear term associated with various nonlinearities of the pipe system. In the following calculations, a four-mode Galerkin approximation will be utilized ($N = 4$) because the instability of the pipe system is usually associated with the lowest several modes.

By neglecting the nonlinear terms in Eq. (7), the eigenvalues of the pipe with IDVA can be obtained. According to the obtained eigenvalues for each mode, the stability of the pipe with the IDVA can be evaluated. When the dimensionless inerter in Eq. (7) is set as $\theta = 0$ and the nonlinear term \mathbf{f}_{nonl} is absent, the eigenvalues of the pipe with DVA may be obtained, referring to [31]. The nonlinear oscillations of the pipe with IDVA can be predicted by numerically solving the nonlinear governing equations via a fourth-order Runge–Kutta iteration algorithm.

4 Results

In this section, the effect of IDVA on the dynamical stability and nonlinear responses of the pipe system is explored. For that purpose, the evolution of eigenvalues for the pipe and the attached mass as a function of the flow velocity will be shown first. Based on the stability analysis of the linear system, the nonlinear oscillations of the pipe and the attached mass will be further studied. Results for the dynamical behaviors of the cantilevered pipe and the attached IDVA for various system parameters will be presented mainly in the form of Argand diagrams, bifurcation diagrams and displacement-time diagrams.

4.1 Model Validation and Simple Comparison

The Argand diagram of a cantilevered fluid-conveying pipe without IDVA for $\phi = 0.001$ and $\beta = 0.213$ is reproduced first to check the correctness of our approximately analytical solutions. The evolution of lowest four eigenvalues of the pipe without IDVA with increasing dimensionless flow velocity, u , is illustrated in Fig. 2. In this figure, it should be noted that $\text{Re}(\omega)$ is the dimensionless oscillation frequency, while $\text{Im}(\omega)$ is related to the dimensionless damping of the whole system. It is obvious that the flutter instability of the pipe occurs in the second mode, at $u_{cr} \approx 5.8$. It is also seen that the results plotted in Fig. 2 agree well with those obtained by Gregory et al. [45] and Paidoussis et al. [46], demonstrating that the approximately analytical solutions obtained in this work are reliable.

In order to explore the effect of IDVA on the basic dynamics of the fluid-conveying cantilever, typical results of Argand diagrams for a cantilevered pipe conveying fluid with DVA and IDVA are shown in Figs. 3 and 4. It is seen from Fig. 3 that flutter instability of the pipe with DVA occurs at $u_{cr} \approx 6.4$. This dimensionless critical flow velocity is much larger than that shown in Fig. 2, indicating that the DVA can improve the stability of the pipe system. It is also noted from Fig. 3 that the present result for the pipe with DVA agrees well with that reported in [31]. Furthermore, as shown in Fig. 4, once the inerter is added to the spring-mass attachment, the dimensionless critical flow velocity of the pipe system would increase further to $u_{cr} \approx 6.9$.

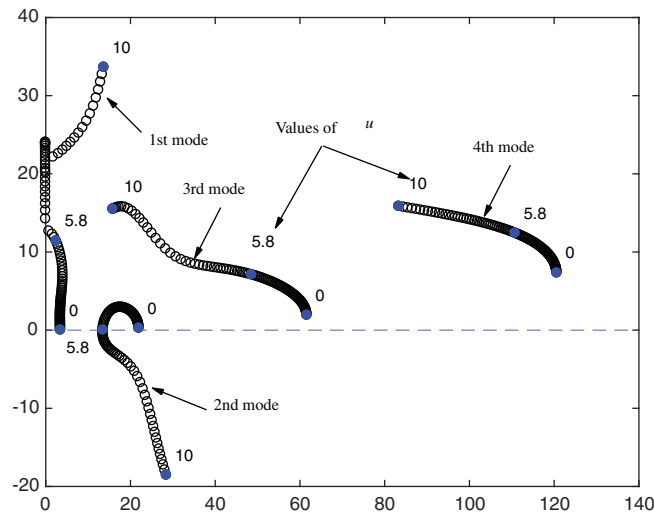


Figure 2: Argand diagram for a cantilevered pipe conveying fluid without IDVA, from which it is seen that the critical flow velocity is about $u_{cr} = 5.8$

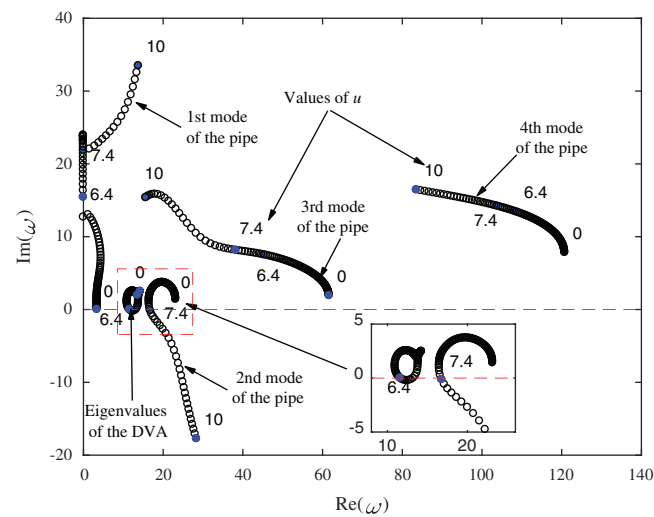


Figure 3: Argand diagram for a cantilevered pipe conveying fluid with DVA for $k = 20$, $c = 0.5$, $\phi = 0.001$, $\alpha = 0.1$, $\beta = 0.213$, $\xi_b = 0.5$. It is seen that the critical flow velocity for the whole system is about $u_{cr} = 6.4$

In order to make the calculation results easier to understand, the dimensional values of critical flow velocity for the pipe with IDVA or without IDVA are briefly discussed. Taking a silicone tube [47] as an example, several key physical and geometrical parameters are chosen as: the flexural rigidity of the pipe $EI = 0.0217 \text{ Nm}^2$, the mass of the empty pipe per unit length $m = 0.19 \text{ kg/m}$, the density of the internal fluid per unit length $\rho = 1000 \text{ kg/m}^3$, the pipe length $L = 0.35 \text{ m}$, the outer diameter $D = 0.0155 \text{ m}$, and the inner diameter of the pipe $d = 0.00794 \text{ m}$. According to the definition of the dimensionless flow velocity $u = [M / (EI)]^{1/2} UL$, the dimensional critical flow velocity of the pipe with IDVA is found to be about $U_{cr} = 7.78 \text{ m/s}$.

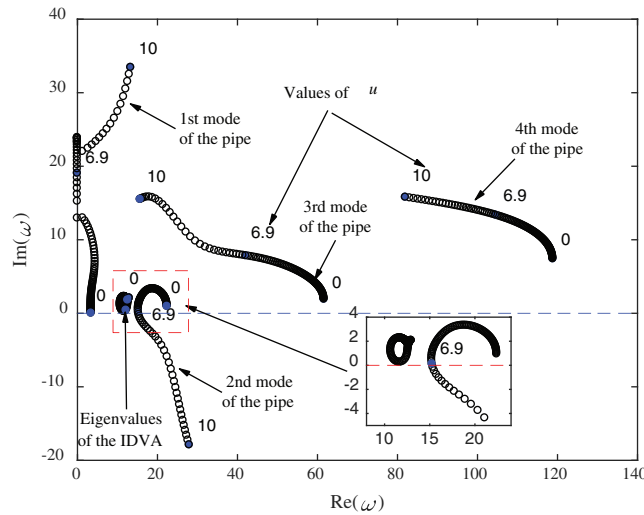


Figure 4: Argand diagram for a cantilevered pipe conveying fluid with IDVA for $k = 20$, $c = 0.5$, $\phi = 0.001$, $\alpha = 0.1$, $\theta = 0.02$, $\beta = 0.213$, $\xi_b = 0.5$. It is seen that the critical flow velocity for the whole system is about $u_{cr} = 6.9$

4.2 Effect of IDVA on the Critical Flow Velocity

In this subsection, the stability of the cantilevered fluid-conveying pipe for various system parameters of the IDVA will be investigated. Figs. 5–12 show the critical flow velocities of the pipe system for various physical and geometrical parameters of the IDVA. In these figures, unless otherwise stated, the system parameters were chosen as: $\phi = 0.001$, $\alpha = 0.1$, $\beta = 0.213$, $\theta = 0.02$, $k = 20$, $c = 0.5$ and $\xi_b = 0.5$.

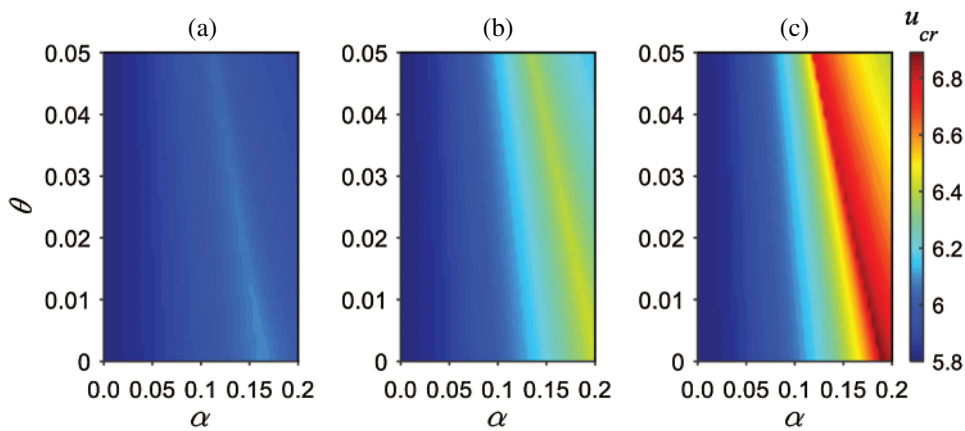


Figure 5: Dimensionless critical flow velocities u_{cr} of the system as a function of dimensionless inerter and mass ratio of the IDVA for $\phi = 0.001$, $k = 28$, $\beta = 0.213$, $\xi_b = 0.5$: (a) $c = 0.1$, (b) $c = 0.3$ and (c) $c = 0.5$

The dimensionless critical flow velocities u_{cr} of the pipe system as a function of dimensionless inerter and mass ratio of the IDVA for $\phi = 0.001$, $k = 28$, $\beta = 0.213$, $\xi_b = 0.5$ are indicated in Fig. 5. The results shown in this figure demonstrate that the critical flow velocities of the

dynamical system increase with the increase of the damping coefficient. As shown in Figs. 5a–5c, with the increase of dimensionless mass ratio, a smaller value of dimensionless inerter of the IDVA is required to achieve higher critical flow velocity.

Fig. 6 shows that the critical flow velocities of the pipe system as a function of dimensionless inerter and mass ratio for three different values of IDVA location (ξ_b). It is found that the critical flow velocities of the system in the case of $\xi_b = 0.75$ change slightly only. The peak value of the critical flow velocity of the dynamical system occurs at $\xi_b \approx 0.5$, as can be seen in Figs. 6a–6c.

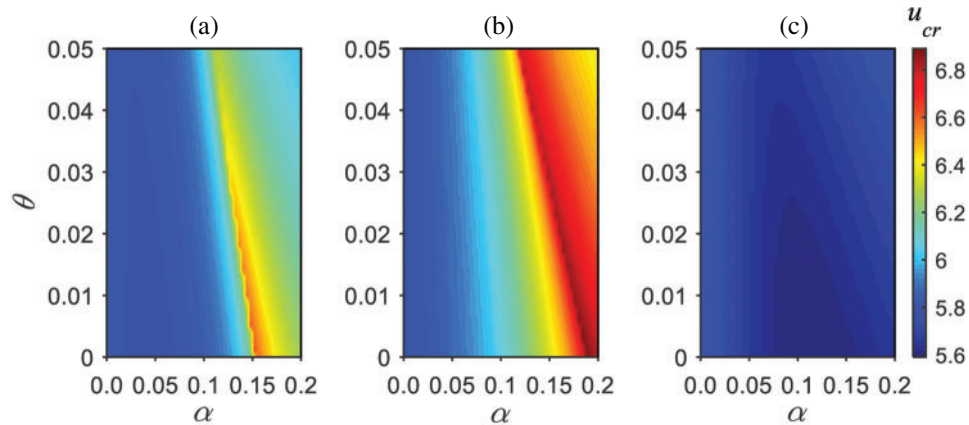


Figure 6: Dimensionless critical flow velocities u_{cr} of the system as a function of dimensionless inerter and mass ratio of the IDVA for $\phi = 0.001$, $k = 28$, $c = 0.5$, $\beta = 0.213$: (a) $\xi_b = 0.25$, (b) $\xi_b = 0.5$ and (c) $\xi_b = 0.75$

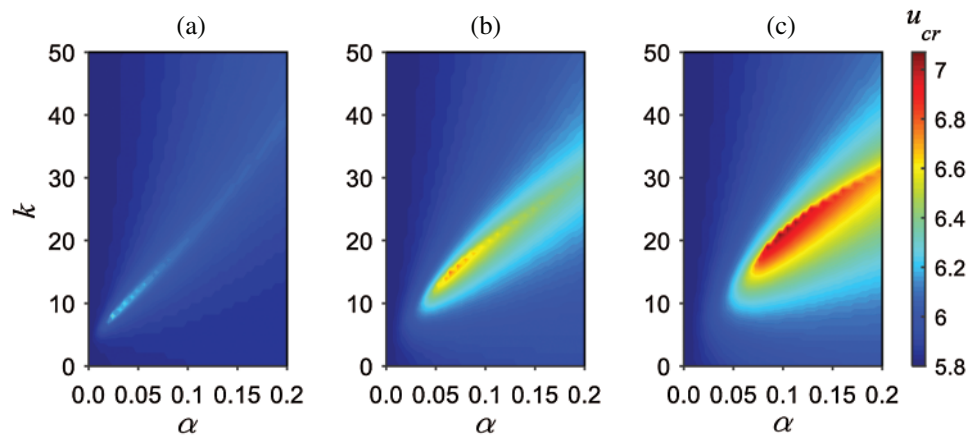


Figure 7: Dimensionless critical flow velocities u_{cr} of the system as a function of dimensionless stiffness and mass ratio of the IDVA for $\phi = 0.001$, $\theta = 0.02$, $\beta = 0.213$, $\xi_b = 0.5$: (a) $c = 0.1$, (b) $c = 0.3$ and (c) $c = 0.5$

Fig. 7 shows that the critical flow velocities of the pipe system as a function of dimensionless stiffness and mass ratio of the IDVA, for three different values of damping coefficient (c). It is obvious that the peak value of the critical flow velocity increases with the increase of damping

coefficient. As shown in Figs. 7a–7c, with the increase of dimensionless damping coefficient of the IDVA, the cantilevered pipe conveying fluid with IDVA can achieve higher critical flow velocity.

The critical flow velocities of the pipe system as a function of dimensionless stiffness and mass ratio of the IDVA are shown in Fig. 8, for three given values of inerter (θ). By inspecting Figs. 8a–8c, a remarkable feature can be found: with the increase of the inerter of IDVA, the critical flow velocities of the pipe with IDVA would reduce. That is to say, a larger value of inerter is detrimental to the system’s stability.

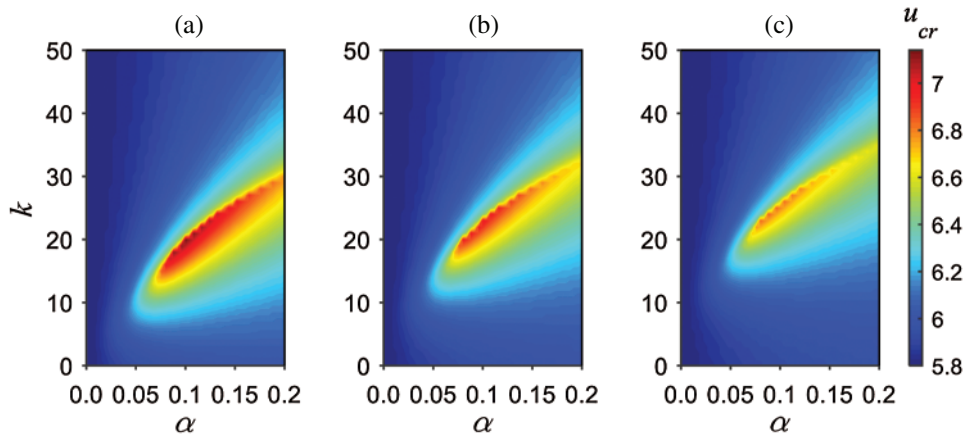


Figure 8: Dimensionless critical flow velocities u_{cr} of the system as a function of dimensionless stiffness and mass ratio of the IDVA for $\phi = 0.001$, $c = 0.5$, $\beta = 0.213$, $\xi_b = 0.5$: (a) $\theta = 0.01$, (b) $\theta = 0.03$ and (c) $\theta = 0.05$

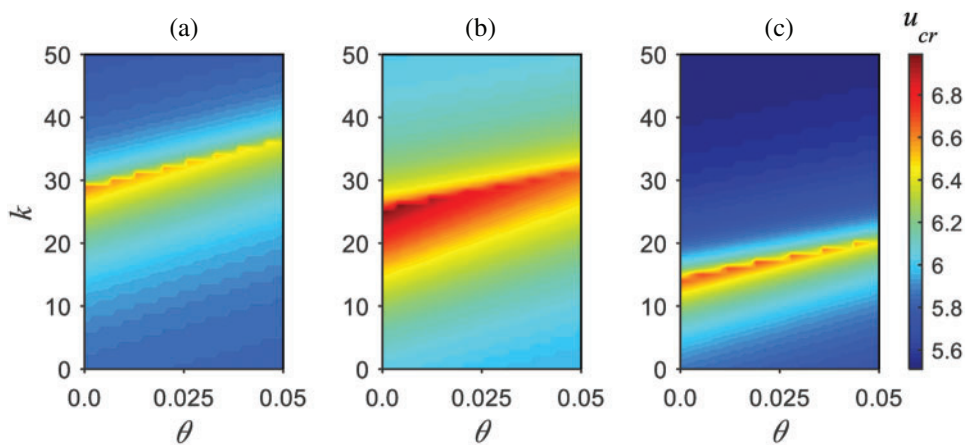


Figure 9: Dimensionless critical flow velocities u_{cr} of the system as a function of dimensionless stiffness and inerter of the IDVA for $\phi = 0.001$, $c = 0.5$, $\alpha = 0.16$, $\beta = 0.213$: (a) $\xi_b = 0.25$, (b) $\xi_b = 0.5$ and (c) $\xi_b = 0.75$

Figs. 9a–9c plot the results of critical flow velocities for two independent parameters, stiffness and inerter, with three different values of IDVA location (ξ_b). It is found that when the IDVA location is closer to the free end of the pipe, the stiffness of the IDVA needs to be decreased to

obtain higher critical flow velocity. Among the three cases shown in Figs. 9a–9c, it is noted that the maximum critical flow velocity appears at $\xi_b = 0.5$.

Figs. 10a–10c show the critical flow velocities of the pipe with the IDVA being attached at $\xi_b = 0.5$, for three different values of mass ratio (α). It is observed that with the increase of mass ratio, the stiffness of the IDVA needs to be increased to achieve higher critical flow velocity. Upon comparing the three diagrams of Fig. 10, again, it is found that higher critical flow velocity can be realized in the case of $\alpha = 0.1$.

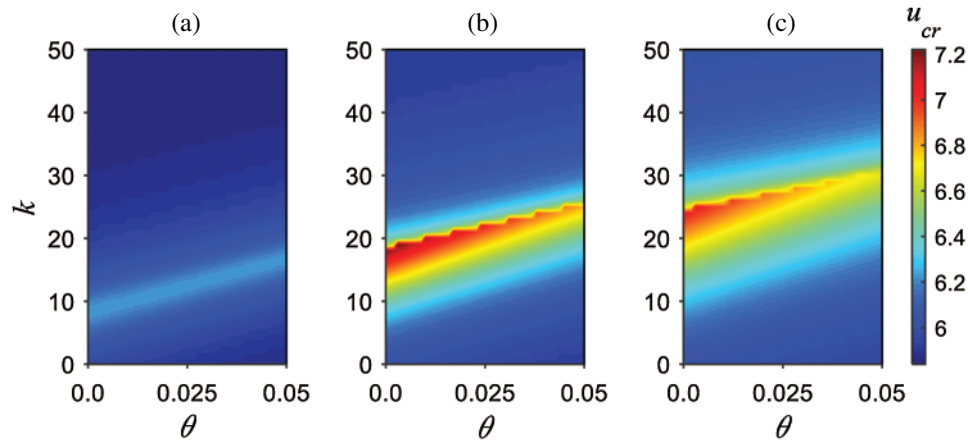


Figure 10: Dimensionless critical flow velocities u_{cr} of the system as a function of dimensionless stiffness and inerter of the IDVA for $\phi = 0.001$, $c = 0.5$, $\beta = 0.213$, $\xi_b = 0.5$: (a) $\alpha = 0.05$, (b) $\alpha = 0.1$ and (c) $\alpha = 0.15$

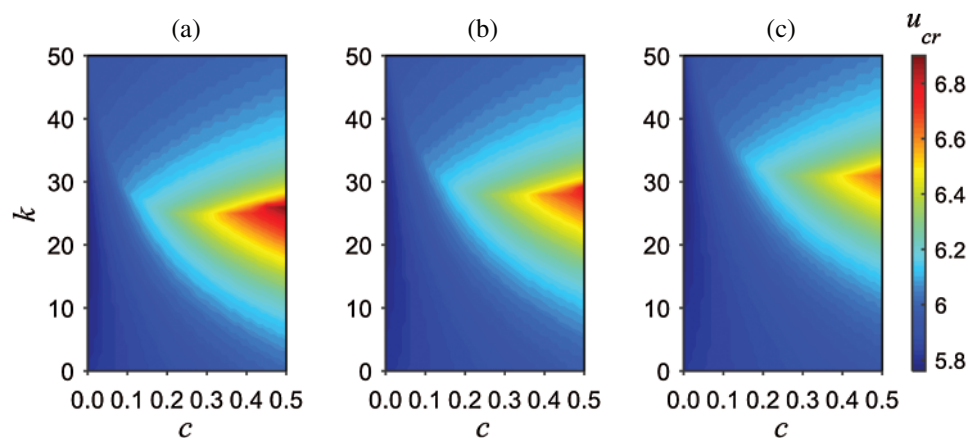


Figure 11: Dimensionless critical flow velocities u_{cr} of the system as a function of dimensionless stiffness and damping of the IDVA for $\phi = 0.001$, $\alpha = 0.16$, $\beta = 0.213$, $\xi_b = 0.5$: (a) $\theta = 0.01$, (b) $\theta = 0.03$ and (c) $\theta = 0.05$

In Fig. 11, the critical flow velocities as a function of dimensionless stiffness and damping coefficient of the IDVA for three different values of inerter are shown. Once again, it is found

that the stability of the pipe can be better enhanced by using the IDVA with smaller values of inerter.

The critical flow velocities of the pipe system as a function of dimensionless stiffness and damping of the IDVA for $\phi = 0.001$, $\theta = 0.02$, $\beta = 0.213$, $\xi_b = 0.5$ and three different values of mass ratio of the IDVA are plotted in Fig. 12. Among the three cases shown in Fig. 12, it is noted that with the increase of mass ratio, the spring stiffness of the IDVA needs to be increased to achieve higher critical flow velocity, and the peak value of the critical flow velocity of the system appears at $\alpha = 0.1$.

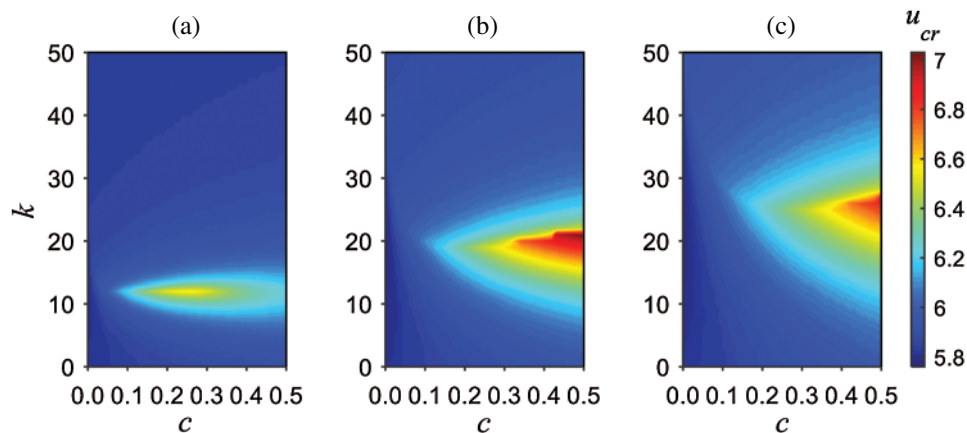


Figure 12: Dimensionless critical flow velocities u_{cr} of the system as a function of dimensionless stiffness and damping of the IDVA for $\phi = 0.001$, $\theta = 0.02$, $\beta = 0.213$, $\xi_b = 0.5$: (a) $\alpha = 0.05$, (b) $\alpha = 0.1$ and (c) $\alpha = 0.15$

4.3 Effect of IDVA on Nonlinear Oscillations of the Pipe

In this subsection, the nonlinear oscillations of the cantilevered pipe conveying fluid with IDVA will be studied when the flow velocity is successively increased. Some fascinating dynamical behaviors will be shown by analyzing this modified system. In order to illustrate the effect of IDVA on the pipe, nonlinear responses of the cantilevered pipe conveying fluid with and without IDVA are examined.

Before embarking some numerical calculations, it is recalled that the argand diagrams for the cantilevered pipe conveying fluid attached with DVA and IDVA show some difference (see Figs. 3 and 4). Therefore, it is expected that the nonlinear responses of the pipe with DVA and with IDVA are also different. To illustrate this, two bifurcation diagrams for the pipe with DVA and with IDVA are plotted in Fig. 13. It is immediately seen that the flutter instability of the pipe with DVA occurs at a higher flow velocity if compared with that of the pipe without IDVA. Furthermore, the pipe with IDVA shows a much higher critical flow velocity. These critical flow velocities for flutter instability based on nonlinear theory are consistent with the linear results shown in Figs. 3 and 4. It is noted that the oscillation amplitudes of the pipe with DVA or with IDVA are generally smaller than that of the plain pipe without any attachments, for a wide range of flow velocity. Interestingly, the pipe with a DVA loses instability at about $u_{cr} = 6.4$, then regains stability at about $u = 7.2$, and finally becomes unstable with further increasing flow velocity. When the flow velocities are higher than $u = 10$, the oscillation amplitudes of the pipe with and without

mass attachment has no obvious difference. The dynamic responses of the DVA and IDVA show similar behaviors as the pipe, which can be observed in Fig. 13b.

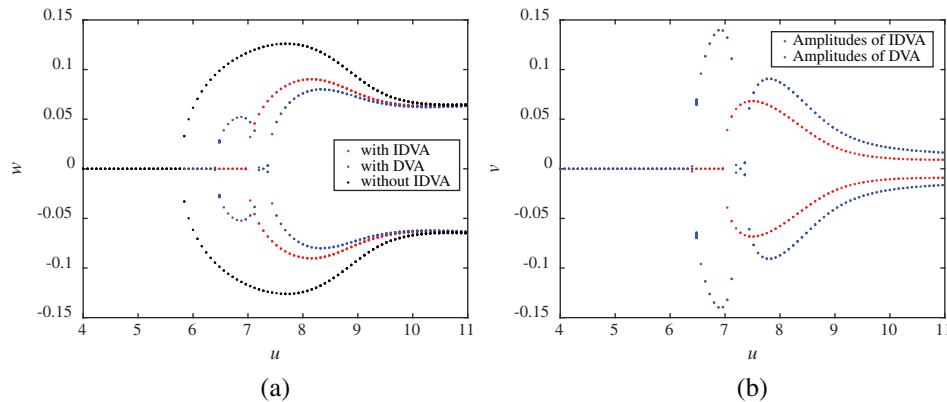


Figure 13: Bifurcation diagrams of the oscillation amplitudes with internal flow velocity u being the variable parameter for: $\phi = 0.001$, $\xi_b = 0.5$, $c = 0.5$, $k = 20$, $\alpha = 0.1$, $\theta = 0.02$, $\beta = 0.213$. (a) Oscillation amplitudes of the pipe at $\xi = 0.5$ and (b) oscillation amplitudes of the IDVA and DVA

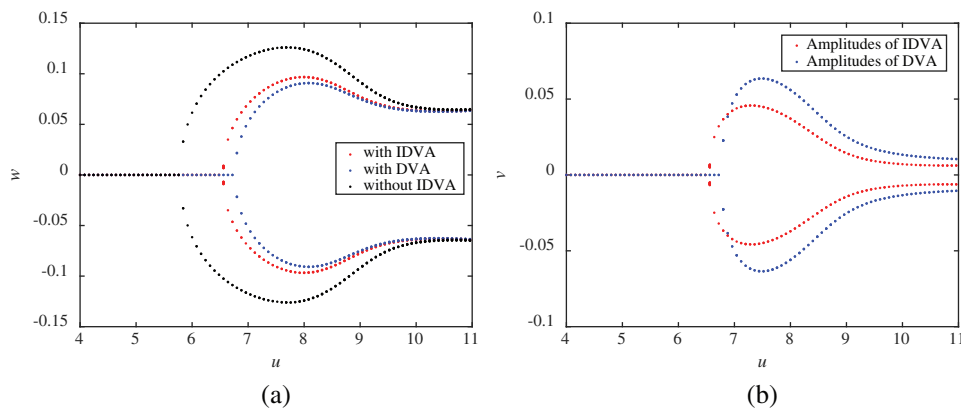


Figure 14: Bifurcation diagrams of the oscillation amplitudes with internal flow velocity u being the variable parameter for: $\phi = 0.001$, $\xi_b = 0.5$, $c = 0.5$, $k = 20$, $\alpha = 0.15$, $\theta = 0.02$, $\beta = 0.213$. (a) Oscillation amplitudes of the pipe at $\xi = 0.5$ and (b) oscillation amplitudes of the IDVA and DVA

When the value of the mass ratio of the IDVA is increased to $\alpha = 0.15$, it is indicated that the dynamical behaviors of the pipe shown in Fig. 14 exhibit some difference from those given in Fig. 13 for $\alpha = 0.1$. It is noted that the pipe with either DVA or IDVA becomes unstable at a critical flow velocity higher than the flow velocity for flutter instability of the pipe without IDVA. One can see that the pipe with DVA for $\alpha = 0.15$ no longer switches between stable and unstable states when the flow velocity is successively increased. Similar phenomenon can be observed in Fig. 14b for the dynamic responses of the IDVA.

In the case of $\alpha = 0.1$ and $\theta = 0.04$, the bifurcation diagrams for the pipe system with flow velocity as the variable parameter are plotted in Fig. 15. It is seen from this figure that the oscillation amplitudes of the pipe with IDVA at the location of the attachment are larger than the counterpart of the pipe with DVA for most flow velocities, while the oscillation amplitudes of the IDVA are generally smaller than that of the DVA. For both cases, the attachment mass can absorb some energy of the whole system, resulting in the decrease of the oscillation amplitudes of the cantilevered pipe.

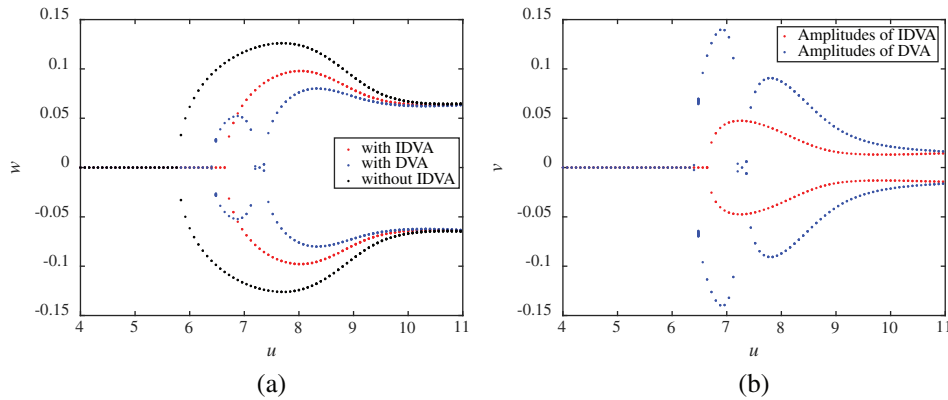


Figure 15: Bifurcation diagrams of the oscillation amplitudes with internal flow velocity u being the variable parameter for: $\phi = 0.001$, $\xi_b = 0.5$, $c = 0.5$, $k = 20$, $\alpha = 0.1$, $\theta = 0.04$, $\beta = 0.213$: (a) displacements of the pipe at $\xi = 0.5$ and (b) displacements of the IDVA and DVA

Bifurcation diagrams of the oscillation amplitudes as a function of the flow velocity for $\phi = 0.001$, $\xi_b = 0.5$, $c = 0.5$, $k = 20$, $\alpha = 0.15$, $\theta = 0.04$, $\beta = 0.213$ are plotted in Fig. 16. In this case, the pipe with DVA has smaller oscillation amplitudes than that of the pipe with IDVA. This implies that the inerter has a negative effect on the vibration suppression of the pipe in such a case.

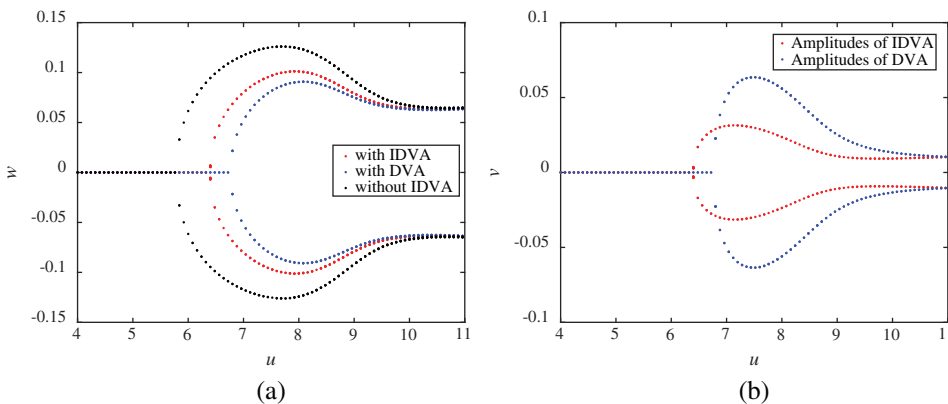


Figure 16: Bifurcation diagrams of the oscillation amplitudes with internal flow velocity u being the variable parameter for: $\phi = 0.001$, $\xi_b = 0.5$, $c = 0.5$, $k = 20$, $\alpha = 0.15$, $\theta = 0.04$, $\beta = 0.213$. (a) Oscillation amplitudes of the pipe at $\xi = 0.5$ and (b) oscillation amplitudes of the IDVA and DVA

The bifurcation diagrams for the pipe system with flow velocity as the variable parameter for $k = 28$, $\alpha = 0.1$ and two different values of inerter are shown in Figs. 17 and 18. It is seen that the critical flow velocity of the pipe with IDVA for $\theta = 0.04$ is slightly larger than that of the pipe with IDVA for $\theta = 0.02$, indicating that the inerter has a positive effect on the stability of the system in this case. It is also observed that, with increasing flow velocity, the oscillation amplitudes of the pipe with IDVA (or DVA) at $\xi = 0.5$ would increase gradually to relatively large values and thereafter decrease to relatively small values. When the flow velocity is sufficiently high (e.g., $u = 10.5$), the oscillation amplitude of the pipe at $\xi = 0.5$ would tend to a constant value.

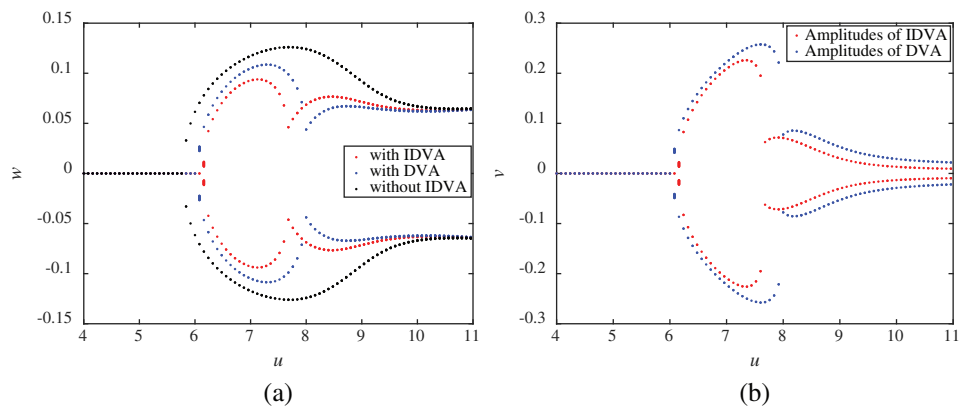


Figure 17: Bifurcation diagrams of the oscillation amplitudes with internal flow velocity u being the variable parameter for: $\phi = 0.001$, $\xi_b = 0.5$, $c = 0.5$, $k = 28$, $\alpha = 0.1$, $\theta = 0.02$, $\beta = 0.213$. (a) Oscillation amplitudes of the pipe at $\xi = 0.5$ and (b) oscillation amplitudes of the IDVA and DVA

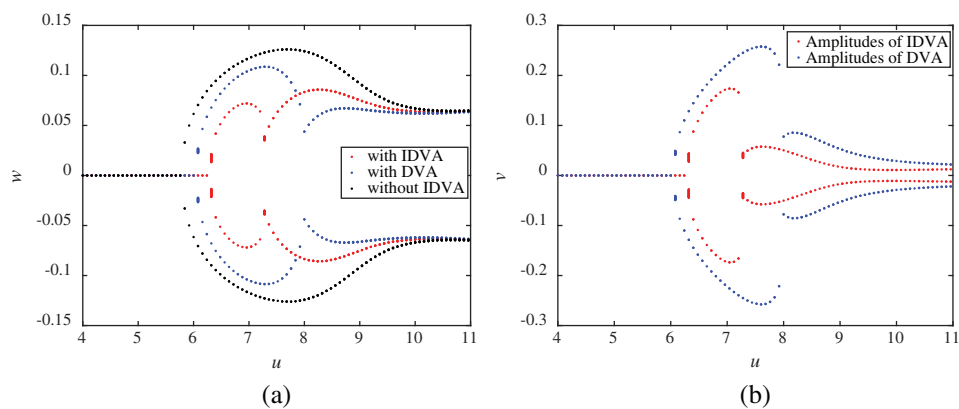


Figure 18: Bifurcation diagrams of the oscillation amplitudes with internal flow velocity u being the variable parameter for: $\phi = 0.001$, $\xi_b = 0.5$, $c = 0.5$, $k = 28$, $\alpha = 0.1$, $\theta = 0.04$, $\beta = 0.213$. (a) Oscillation amplitudes of the pipe at $\xi = 0.5$ and (b) oscillation amplitudes of the IDVA and DVA

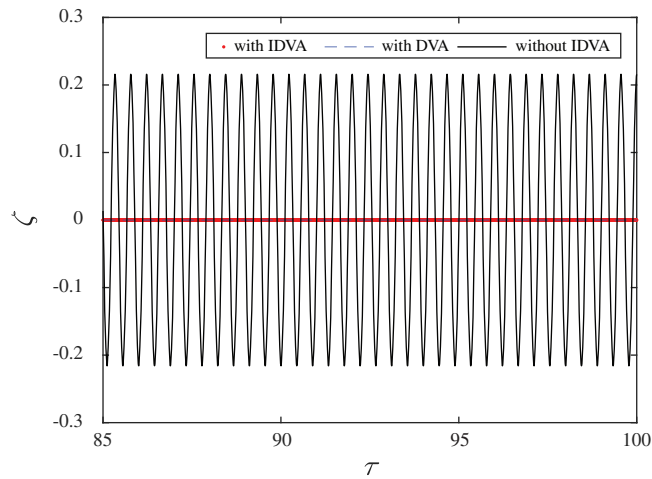


Figure 19: Tip-end displacements of the cantilevered pipe with IDVA, with DVA and without IDVA, for $\phi = 0.001$, $\xi_b = 0.5$, $c = 0.5$, $k = 20$, $\alpha = 0.1$, $\theta = 0.02$, $\beta = 0.213$ and $u = 6.2$

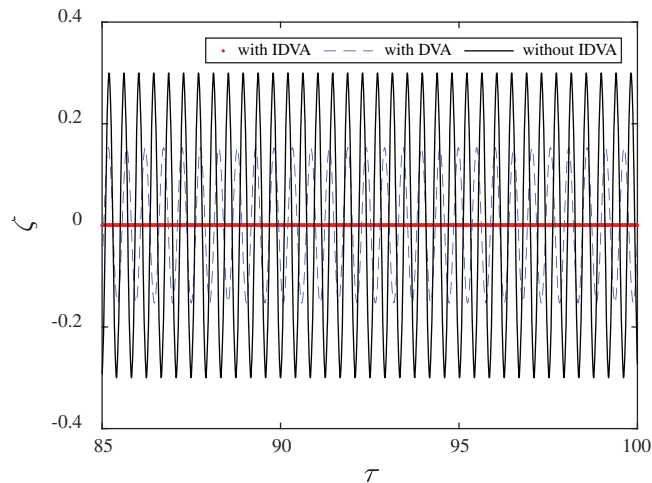


Figure 20: Tip-end displacements of the cantilevered pipe with IDVA, with DVA and without IDVA, for $\phi = 0.001$, $\xi_b = 0.5$, $c = 0.5$, $k = 20$, $\alpha = 0.1$, $\theta = 0.02$, $\beta = 0.213$ and $u = 6.8$

In order to further compare the dynamic responses of the cantilevered pipe conveying fluid with IDVA and without IDVA, some displacement-time curves (time traces) for several typical flow velocities are demonstrated in Figs. 19–22. The displacement-time curves shown in Fig. 19 are for $u = 6.2$. It is obvious that the pipe without IDVA undergoes a periodic oscillation while the displacements of the pipe with DVA or IDVA is towards to zero. In this case, therefore, the pipe with IDVA or DVA becomes more stable than the pipe without IDVA. It is clearly seen from Fig. 20 that the pipe undergoes a periodic motion, either with DVA or without IDVA, while the pipe with IDVA keeps still for $u = 6.8$. Moreover, the oscillation amplitudes of the pipe without IDVA are much larger than the counterpart of the same pipe with DVA. In the case of $u = 7.3$, the displacement-time curves are shown in Fig. 21. It is fascinating that the pipe without and with IDVA occurs flutter instability while the pipe with DVA keeps stable. That is to say, the

pipe with DVA shows a better stability performance than the same pipe but with IDVA in case of $u = 7.3$. When the flow velocity is up to $u = 8$, the result shown in Fig. 22 indicates that the pipe undergoes a periodic motion, even if the pipe is installed with IDVA or DVA. It is also noted that the oscillation amplitude of the pipe without IDVA is larger than that of the pipe with IDVA. Unfortunately, the oscillation amplitude of the pipe with IDVA is larger than that of the pipe with DVA.

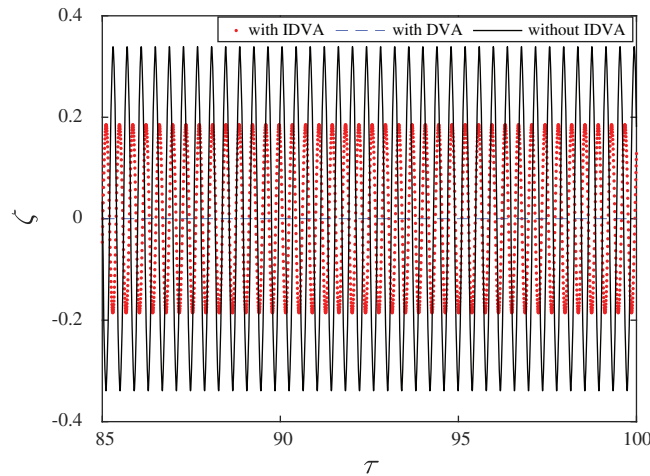


Figure 21: Tip-end displacements of the cantilevered pipe with IDVA, with DVA and without IDVA, for $\phi = 0.001$, $\xi_b = 0.5$, $c = 0.5$, $k = 20$, $\alpha = 0.1$, $\theta = 0.02$, $\beta = 0.213$ and $u = 7.3$

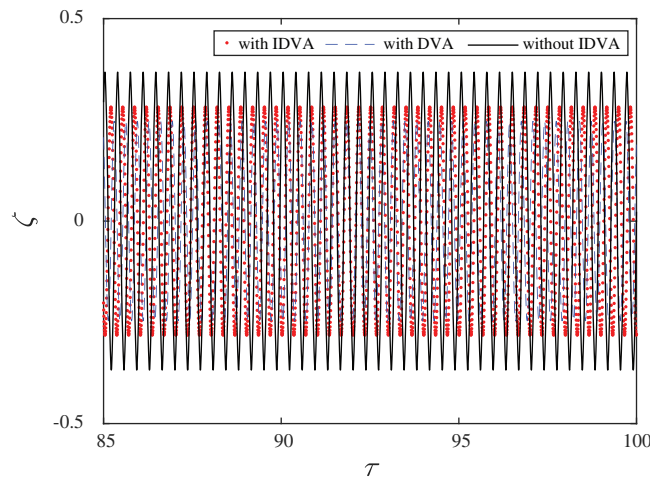


Figure 22: Tip-end displacements of the cantilevered pipe with IDVA, with DVA and without IDVA, for $\phi = 0.001$, $\xi_b = 0.5$, $c = 0.5$, $k = 20$, $\alpha = 0.1$, $\theta = 0.02$, $\beta = 0.213$ and $u = 8$

5 Conclusions

The dynamical stability and nonlinear responses of a cantilevered pipe conveying fluid with an IDVA added somewhere along the pipe length are explored in the present study. For a plain pipe without IDVA, the dynamical system loses stability via flutter when the flow velocity exceeds a certain critical value. For the same pipe but with an IDVA, the flutter instability would occur at a higher critical flow velocity. By constructing Argand diagrams for eigenvalues of the dynamical system, it is found that the damping coefficient, stiffness, location, weight and inerter of the additional IDVA do have effect on the stability of the pipe. Under certain conditions, the critical flow velocity of the pipe can be remarkably increased by adding the IDVA, and hence the stability of the pipe can be enhanced. The underlying reason of the enhanced stability of the fluid-conveying pipe is associated with the transfer of energy from the pipe to the IDVA. To evaluate the effect of IDVA on the nonlinear behaviors of the pipe, the oscillations of the pipe and the IDVA are also calculated based on nonlinear theories. It is shown that the oscillation amplitudes of the pipe with IDVA are sometimes smaller than that of the pipe with DVA, and the oscillation amplitudes of the IDVA are always larger than that of the DVA. Therefore, the results obtained in this paper may be expected to be useful for the design of energy absorbers (or energy transfer devices) of fluid-conveying pipes by adding IDVAs somewhere along the pipe length. However, this does not mean that the IDVA is always better than a DVA for enhancing the stability and suppressing the oscillations of cantilevered pipes conveying fluid. Within some ranges of flow velocity, indeed, the DVA has a better performance, as shown in [Figs. 13–18](#).

Furthermore, for a pipe with both ends positively supported, buckling is the preferred form of instability since it is a conservative system in the absence of dissipation. When an inerter-based DVA is added to the supported pipe, the linear spring of the IDVA could change the effective bending stiffness of the whole pipe system. For this reason, it can be foreseen that the IDVA can affect the stability of pipes with both ends supported.

Funding Statement: The authors gratefully acknowledge the support provided by the National Natural Science Foundation of China (Nos. 11622216, 11672115 and 11972167).

Conflicts of Interest: The authors declare that they have no conflicts of interest to report regarding the present study.

References

1. Tang, Y., Yang, T., Fang, B. (2018). Fractional dynamics of fluid-conveying pipes made of polymer-like materials. *Acta Mechanica Solida Sinica*, 31(2), 243–258. DOI 10.1007/s10338-018-0007-9.
2. Yau, C. H., Bajaj, A. K., Nwokah, O. D. I. (1995). Active control of chaotic vibration in a constrained flexible pipe conveying fluid. *Journal of Fluids and Structures*, 9(1), 99–122. DOI 10.1006/jfls.1995.1005.
3. Deng, Q. T., Yang, Z. C. (2019). Wave propagation in submerged pipe conveying fluid. *Acta Mechanica Solida Sinica*, 32(4), 483–498. DOI 10.1007/s10338-019-00090-x.
4. Wang, L., Zhong, Z. (2018). Complex modal analysis for the time-variant dynamical problem of rotating pipe conveying fluid. *Computer Modeling in Engineering & Sciences*, 114(1), 1–18.
5. Li, Q., Liu, W., Lu, K., Yue, Z. (2020). Nonlinear parametric vibration of a fluid-conveying pipe flexibly restrained at the ends. *Acta Mechanica Solida Sinica*, 33(3), 327–346. DOI 10.1007/s10338-019-00147-x.
6. Askarian, A., Permoon, M., Shakouri, M. (2020). Vibration analysis of pipes conveying fluid resting on a fractional Kelvin–Voigt viscoelastic foundation with general boundary conditions. *International Journal of Mechanical Sciences*, 179, 105702. DOI 10.1016/j.ijmecsci.2020.105702.

7. Koo, G. H., Park, Y. S. (1998). Vibration reduction by using periodic supports in a piping system. *Journal of Sound and Vibration*, 210(1), 53–68. DOI 10.1006/jsvi.1997.1292.
8. Chen, S. S., Jendrzejczyk, J. A. (1985). General characteristics, transition, and control of instability of tubes conveying fluid. *Journal of the Acoustical Society of America*, 77(3), 887–895. DOI 10.1121/1.392057.
9. Tsai, Y. K., Lin, Y. H. (1997). Adaptive modal vibration control of a fluid-conveying cantilever pipe. *Journal of Fluids and Structures*, 11(5), 535–547. DOI 10.1006/jfls.1997.0092.
10. Demir, M. H., Yesildirek, A., Yigit, F. (2015). Control of a cantilever pipe conveying fluid using neural network. *6th International Conference on Modeling, Simulation, and Applied Optimization*, pp. 1–6. Istanbul.
11. Elvin, N. G., Elvin, A. A. (2009). The flutter response of a piezoelectrically damped cantilever pipe. *Journal of Intelligent Material Systems and Structures*, 20(16), 2017–2026. DOI 10.1177/1045389X09345557.
12. Tani, J. J. (1992). Active flutter suppression of a tube conveying fluid. *First European Conference on Smart Structures and Materials*, pp. 333–336. Glasgow. DOI 10.1117/12.2298093.
13. Tani, J., Sudani, Y. (1995). Active flutter suppression of a vertical pipe conveying fluid. *JSME International Journal: Series C, Dynamics, Control, Robotics, Design and Manufacturing*, 38(1), 55–58. DOI 10.1299/jsmec1993.38.55.
14. Lin, Y. H., Chu, C. L. (1996). Active flutter control of a cantilever tube conveying fluid using piezoelectric actuators. *Journal of Sound and Vibration*, 196(1), 97–105. DOI 10.1006/jsvi.1996.0470.
15. Lin, Y. H., Tsai, Y. K. (1997). Non-linear active vibration control of a cantilever pipe conveying fluid. *Journal of Sound and Vibration*, 202(4), 477–490. DOI 10.1006/jsvi.1996.0858.
16. Khajepour, S., Azadi, V. (2015). Vibration suppression of a rotating flexible cantilever pipe conveying fluid using piezoelectric layers. *Latin American Journal of Solids and Structures*, 12(6), 1042–1060. DOI 10.1590/1679-78251535.
17. Hussein, D. S., Al-Waily, M. (2019). Active vibration control analysis of pipes conveying fluid rested on different supports using state-space method. *International Journal of Energy and Environment*, 10(6), 329–344.
18. Jordanov, I. N., Cheshankov, B. I. (1988). Optimal design of linear and non-linear dynamic vibration absorbers. *Journal of Sound and Vibration*, 123(1), 157–170. DOI 10.1016/S0022-460X(88)80085-3.
19. Yoshizawa, M., Suzuki, T., Takayanagi, M., Hashimoto, K. (1998). Nonlinear lateral vibration of a vertical fluid-conveying pipe with end mass (special issue on nonlinear dynamics). *JSME International Journal Series C*, 41(3), 652–661. DOI 10.1299/jsmec.41.652.
20. Hiramoto, K., Doki, H. (2004). Simultaneous optimal design of structural and control systems for cantilevered pipes conveying fluid. *Journal of Sound and Vibration*, 274(3–5), 685–699. DOI 10.1016/S0022-460X(03)00745-4.
21. Rinaldi, S., Paidoussis, M. P. (2010). Dynamics of a cantilevered pipe discharging fluid, fitted with a stabilizing end-piece. *Journal of Fluids and Structures*, 26(3), 517–525. DOI 10.1016/j.jfluidstructs.2010.01.004.
22. Wang, L., Dai, H. L. (2012). Vibration and enhanced stability properties of fluid-conveying pipes with two symmetric elbows fitted at downstream end. *Archive of Applied Mechanics*, 82(2), 155–161. DOI 10.1007/s00419-011-0545-9.
23. Wang, Z. M., Feng, Z. Y., Zhao, F. Q., Liu, H. Z. (2000). Analysis of coupled-mode flutter of pipes conveying fluid on the elastic foundation. *Applied Mathematics and Mechanics*, 21(10), 1177–1186. DOI 10.1007/BF02458996.
24. Doaré, O., de Langre, E. (2002). Local and global instability of fluid-conveying pipes on elastic foundations. *Journal of Fluids and Structures*, 16(1), 1–14. DOI 10.1006/jfls.2001.0405.
25. Pisarski, D., Konowrocki, R., Szmidt, T. (2018). Dynamics and optimal control of an electromagnetically actuated cantilever pipe conveying fluid. *Journal of Sound and Vibration*, 432, 420–436. DOI 10.1016/j.jsv.2018.06.045.

26. Yang, T. Z., Yang, X. D., Li, Y. H., Fang, B. (2013). Passive and adaptive vibration suppression of pipes conveying fluid with variable velocity. *Journal of Vibration and Control*, 20(9), 1293–1300. DOI 10.1177/1077546313480547.
27. Mamaghani, A. E., Khadem, S. E., Bab, S. (2016). Vibration control of a pipe conveying fluid under external periodic excitation using a nonlinear energy sink. *Nonlinear Dynamics*, 86(3), 1761–1795. DOI 10.1007/s11071-016-2992-x.
28. Song, G. B., Zhang, P., Li, L. et al. (2016). Vibration control of a pipeline structure using pounding tuned mass damper. *Journal of Engineering Mechanics*, 142(6), 04016031. DOI 10.1061/(ASCE)EM.1943-7889.0001078.
29. Rechenberger, S., Mair, D. (2017). Vibration control of piping systems and structures using tuned mass dampers. *ASME 2017 Pressure Vessels and Piping Conference*, Hawaii, USA.
30. Zhou, K., Xiong, F. R., Jiang, N. B., Dai, H. L., Yan, H. et al. (2018). Nonlinear vibration control of a cantilevered fluid-conveying pipe using the idea of nonlinear energy sink. *Nonlinear Dynamics*, 95(2), 1435–1456. DOI 10.1007/s11071-018-4637-8.
31. Liu, Z. Y., Zhou, K., Wang, L., Jiang, T. L., Dai, H. L. (2019). Dynamical stability of cantilevered pipe conveying fluid in the presence of linear dynamic vibration absorber. *Journal of Computational Applied Mechanics*, 50, 182–190.
32. Brzeski, P., Pavlovskaja, E., Kapitaniak, T., Perlikowski, P. (2015). The application of inerter in tuned mass absorber. *International Journal of Non-Linear Mechanics*, 70, 20–29. DOI 10.1016/j.ijnonlinmec.2014.10.013.
33. Hu, Y., Chen, M. Z. Q. (2015). Performance evaluation for inerter-based dynamic vibration absorbers. *International Journal of Mechanical Sciences*, 99, 297–307. DOI 10.1016/j.ijmecsci.2015.06.003.
34. Hu, Y., Chen, M. Z. Q., Xu, S., Liu, Y. (2017). Semiactive inerter and its application in adaptive tuned vibration absorbers. *IEEE Transactions on Control Systems Technology*, 25(1), 294–300. DOI 10.1109/TCST.2016.2552460.
35. Zhang, Y. W., Lu, Y. N., Zhang, W., Teng, Y. Y., Yang, H. X. (2019). Nonlinear energy sink with inerter. *Mechanical Systems and Signal Processing*, 125, 52–64. DOI 10.1016/j.ymssp.2018.08.026.
36. Liang, F., Yang, X. D. (2020). Wave properties and band gap analysis of deploying pipes conveying fluid with periodic varying parameters. *Applied Mathematical Modelling*, 77, 522–538. DOI 10.1016/j.apm.2019.07.064.
37. Liang, F., Gao, A., Yang, X. D. (2020). Dynamical analysis of spinning functionally graded pipes conveying fluid with multiple spans. *Applied Mathematical Modelling*, 83, 454–469. DOI 10.1016/j.apm.2020.03.011.
38. Semler, C. (1922). *Nonlinear dynamics and chaos of a pipe conveying fluid (Ph.D. Thesis)*. McGill University, Canada.
39. Liu, Z. Y. (2019). *Nonlinear vibration and passive control of fluid-conveying cantilevered pipe (Ph.D. Thesis)*. Huazhong University of Science and Technology, China (in Chinese).
40. Liu, Z. Y., Jiang, T. L., Wang, L., Dai, H. L. (2019). Nonplanar flow-induced vibrations of a cantilevered PIP structure system concurrently subjected to internal and cross flows. *Acta Mechanica Sinica*, 35(6), 1241–1256. DOI 10.1007/s10409-019-00879-6.
41. Liu, Z. Y., Wang, L., Dai, H. L., Wu, P., Jiang, T. L. (2019). Nonplanar vortex-induced vibrations of cantilevered pipes conveying fluid subjected to loose constraints. *Ocean Engineering*, 178, 1–19. DOI 10.1016/j.oceaneng.2019.02.070.
42. Shen, Y. H., Liu, C. S. (2011). A new insight into the differential quadrature method in solving 2-D elliptic PDEs. *Computer Modeling in Engineering & Sciences*, 71(2), 157–178.
43. Li, H., Mulay, S. S., See, S. (2009). On the location of zeroes of polynomials from the stability analysis of novel strong-form meshless random differential quadrature method. *Computer Modeling in Engineering and Sciences*, 54(2), 147–200.
44. Wang, L., Ni, Q. (2008). In-plane vibration analyses of curved pipes conveying fluid using the generalized differential quadrature rule. *Computers & Structures*, 86(1), 133–139. DOI 10.1016/j.compstruc.2008.02.007.

45. Gregory, R. W., Paidoussis, M. P. (1966). Unstable oscillation of tubular cantilevers conveying fluid I. theory. *Proceedings of the Royal Society of London. Series A. Mathematical and Physical Sciences*, 293(1435), 512–527. DOI 10.1098/rspa.1966.0187.
46. Paidoussis, M. P., Issid, N. T. (1974). Dynamic stability of pipes conveying fluid. *Journal of Sound and Vibration*, 33(3), 267–294. DOI 10.1016/S0022-460X(74)80002-7.
47. Paidoussis, M. P., Moon, F. C. (1988). Nonlinear and chaotic fluidelastic vibrations of a flexible pipe conveying fluid. *Journal of Fluids and Structures*, 6(2), 567–591. DOI 10.1016/S0889-9746(88)80023-9.